CHAPTER IV

THE EFFECTS OF FIRING TEMPERATURES AND DWELL TIME ON PHASE FORMATION, MICROSTRUCTURE AND DIELECTRIC PROPERTIES OF $BaZr_{0.10}Ti_{0.90}O_3$ CERAMICS PREPARED VIA THE COMBUSTION TECHNIQUE

Introduction

$Ba(Zr_xTi_{1-x})O_3$ ceramics are a solid solution of $BaTiO_3$ and $BaZrO_3$. These ceramics have been studied widely due to their very high and broad dielectric constant, excellent tunability and because they are environmentally friendly materials [5]. The ferroelectric properties of these materials are largely dependent on the amount of Zr substitution [6]. Normal ferroelectric behavior and good dielectric properties, with the Curie temperature above room temperature, where exhibited when $0 < x < 0.2$. When $x > 0.3$, relaxor behavior was observed and the Curie temperature went below room temperature [3]. In the case of $Ba(Zr_{0.1}Ti_{0.9})O_3$ (abbreviated as BZT10) ceramics, it is of great interest due to its high dielectric constant, low dielectric loss, wide dielectric curve and a Curie temperature above room temperature [7, 8]. This makes it promising for use in various applications such as: a storage capacitor for the next DRAM generation and a dielectric material for multilayer chip ceramic capacitors [7].

BZT10 ceramics can prepare by several methods such as: solid-state reaction [8], the sol-gel route [9] and the co-precipitation technique [7]. Kuang, et al. [8] prepared BZT by solid-state reaction using a calcined temperature of 1100 °C for 2 h and a sintering temperature of 1400 °C for 4 h. The maximum density of the ceramics was found at around 95% and the maximum dielectric constant was 12,500 at 10 kHz. To reduce the sintering temperature, Binhayeeniyi, et al. [9] synthesized BZT10 ceramics via the sol-gel route. Dried gel was calcined at 1100 °C for 2 h and a powder with an average particle size of around 0.29 mm was obtained. After being sintered at 1250 °C, the results showed a density of around 84% and a maximum dielectric constant value of 8500. BZT10 nano-powders were successfully obtained by the aqueous co-precipitation method [7]. NaOH with 15M concentrations was used for

precipitation and when the pH was maintained over 12, nano-powders of BZT10 (~30 nm) were obtained. After sintering at 1600 °C for 4 h, maximum density and maximum dielectric constant of 96% and 11,000 of BZT10 ceramics were obtained. It is well known that, a solid-state reaction is relatively simple, yet it is time consuming, energy intensive, and the calcined powders are often large and inhomogeneous [20]. While the wet chemicals can provide ultra-fine and more homogeneous powders, these methods require a longer processing time, require expensive chemicals, special equipment and have a complex procedure [21].

Recently, the combustion technique has become an attractive technique to prepare ferroelectric ceramics [20, 21, 52, 53]. It is an uncomplicated technique which provides high quality ceramics. The combustion reaction provides heat that can be effectively applied to the raw materials. This energy speeds up the chemical reaction of the materials [22] which produces pure nanocrystalline powders [23, 24], a high density [24, 54] and good electrical properties [55, 56] with lower firing temperatures and shorter dwell time compared to the conventional method [52, 53]. Furthermore, it is well known that firing conditions strongly influence phase formation, microstructure and the dielectric properties of calcined powders and sintered ceramics. For instant, the lattice parameter *c* and the tetragonality (*c/a*) tend to decrease while the lattice parameter a increases with increasing firing temperatures [57, 58]. The crystallite size increases and the particle morphology changes from spherical to cube-shaped with increasing calcination temperatures [59]. The optimum sintering temperature also provides the highest density and the maximum dielectric constant [55, 57]. However, no researcher has reported the preparation of BZT10 ceramics by the combustion technique and no one has shown the results of firing conditions on phase formation, microstructure and the dielectric properties of BZT10 ceramics. Therefore, in this work, BZT10 ceramics prepared by the combustion technique were studied. The effects of calcination temperatures, sintering temperatures and dwell time on phase, morphology and electric permittivity evolution of perovskite BZT10 was investigated.

Experimental procedure

BZT10 was prepared via the combustion technique using urea as fuel. High purity powders of barium carbonate ($BaCO_3$), zirconium dioxide (ZrO_2) and titanium

dioxide (TiO_2) were used as starting materials for the $Ba(Zr_{0.1}Ti_{0.9})O_3$ ceramics. Starting materials were weighed and mixed by the ball-milling method for 24 h. The suspensions were dried and the powders were ground using an agate mortar and then sieved into a fine powder. The mixed powders and urea (CH_4N_2O) were mixed with a ratio of 1:2 in an agate mortar. After sieving, the reaction of uncalcined powders and urea was investigated by thermogravimetric and differential scanning calorimeter (TGA-DSC) using a heating rate of 10 °C/min from room temperature to 1300 °C. The mixed powders were calcined at various calcination temperatures and dwell times ranging from 600 to 1300 °C for 2-5 h. The calcined powders were pressed into pellets of 15 mm in diameter using uniaxial pressing in a stainless steel mold. The pellets were subsequently sintered between 1300 and 1500 °C with a dwell time of 2 h. X-ray diffraction (XRD) was employed to identify the phase formed and the optimum temperature and dwell time for the $Ba(Zr_{0.1}Ti_{0.9})O_3$ powders and ceramics. SEM photographs were used to observe morphology, the particle size of powders and the grain size of the ceramics. The morphologies of calcined powders were also studied by transmission electron microscopy (TEM). The bulk densities of the sintered samples were measured by the Archimedes method. The dielectric constant (ε_r), dielectric loss ($\tan\delta$) and the transition temperature of the ceramics were measured by an LCR meter.

Chemical compositions reaction

$$BaCO_3 + 0.1ZrO_2 + 0.9TiO_2 \rightarrow Ba(Zr_{0.1}Ti_{0.9})O_3 + CO_2 \qquad \text{[Eq. 19]}$$

Results and discussion

The TGA-DSC curves for investigating range of calcinations temperatures of the mixed powders of $BaCO_3$, ZrO_2, TiO_2 and urea are shown in Figure 39. The TGA results showed three distinct weight losses. The first weight loss occurred between 130 and 235 °C corresponding to endothermic peaks at 136 and 233 °C in the DSC curve. These observations caused from the melting of urea into a liquid phase (melting point of urea is 135 °C). The chemical reaction in this phase consisted of the thermolysis of urea to ammonia (NH_3) and isocyanic acid (HNCO) as shown in Eq.20 [45]. Moreover, the HNCO continuously reacted with the residual water vapor to produce carbon dioxide and ammonia as exhibited in Eq.21 [45]. The second weight loss slowly occurred between 240 and 500 °C corresponding to endothermic peaks at 422

and 492 °C in the DSC curve. These can be attributed to isocyanic acid gradually decomposed to cyanuric acid at 300 °C and cyanuric acid was transformed to isocyanic again at higher temperature as shown in Eq. 22. The complex decomposition reaction of urea released energy, which availed the more activated chemical reaction of raw materials. The third weight loss occurred at temperature higher than 600 °C corresponding to endothermic peaks at 608 and 850 °C in the DSC curve. This can infers the chemical reaction of raw materials was occurred in this stage. These results were used to estimate the calcinations temperature range from 600 to 1300 °C.

$$CO(NH_2)_2 \rightarrow NH_3 + HNCO \qquad \text{[Eq. 20]}$$

$$HNCO + H_2O \rightarrow NH_3 + CO_2 \qquad \text{[Eq. 21]}$$

$$3HNCO \leftrightarrow C_3H_3N_3O_3 \qquad \text{[Eq. 22]}$$

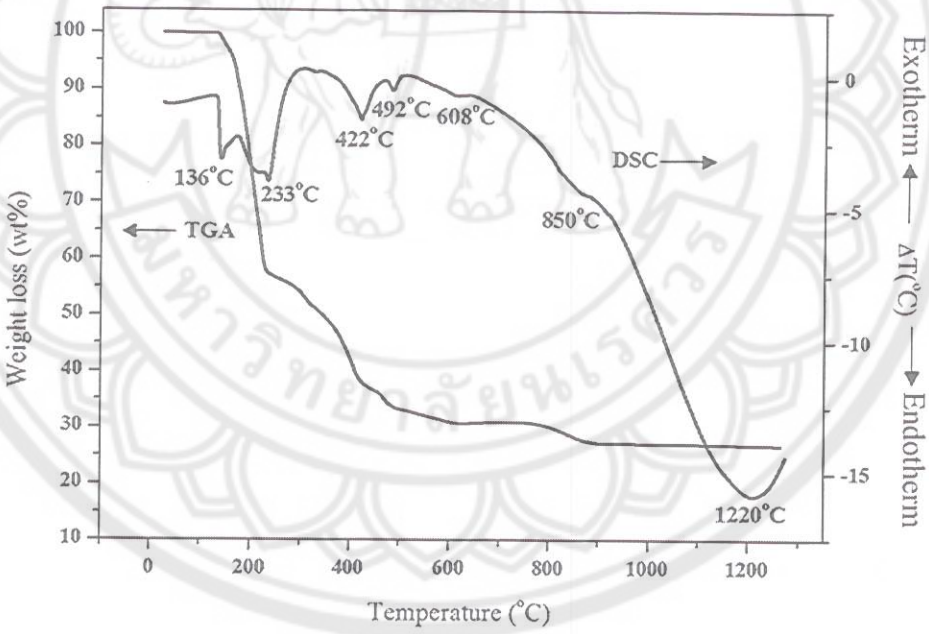

Figure 39 TGA-DSC curves for the mixture of BZT powders and urea

Figure 40 illustrates the XRD patterns of BZT10 powders calcined at various calcination temperatures between 600 and 1300 °C for 2 h. All peaks showed a perovskite structure. The starting materials, such as $BaCO_3$ and ZrO_2, were found in all the calcined powders. Furthermore, the impurity phase of Ba_2TiO_4 was also found

in samples calcined higher 1000 °C. The percentage of the perovskite phase was determined by measuring the major XRD peak intensities using the following equation:

$$\%\text{perovskite phase} = \left(\frac{I_{perov}}{I_{perov} + I_{BaCO_3} + I_{ZrO_2} + I_{Ba_2TiO_4}} \right) \times 100 \qquad \text{[Eq. 23]}$$

This equation is a well-known equation widely employed in connection with the preparation of complex perovskite structure materials [60]. Here I_{perove}, I_{BaCO_3}, I_{ZrO_2} and $I_{Ba_2TiO_4}$ refer to the intensity of the (011) perovskite peak, and the intensities of the highest $BaCO_3$, ZrO_2 and Ba_2TiO_4 peaks, respectively. The percentage of the perovskite phase increased with the increase of calcination temperatures up to 1000°C. Then, the percentage of perovskite tended to decrease with calcination temperatures higher than this temperature (Table 10). The highest percent of the perovskite phase in the BZT10 powder was 96.5%. This was obtained from powder calcined at 1000 °C for 2 h. To achieve the pure perovskite phase, a longer dwell time was performed at a calcinations temperature of 1000 °C.

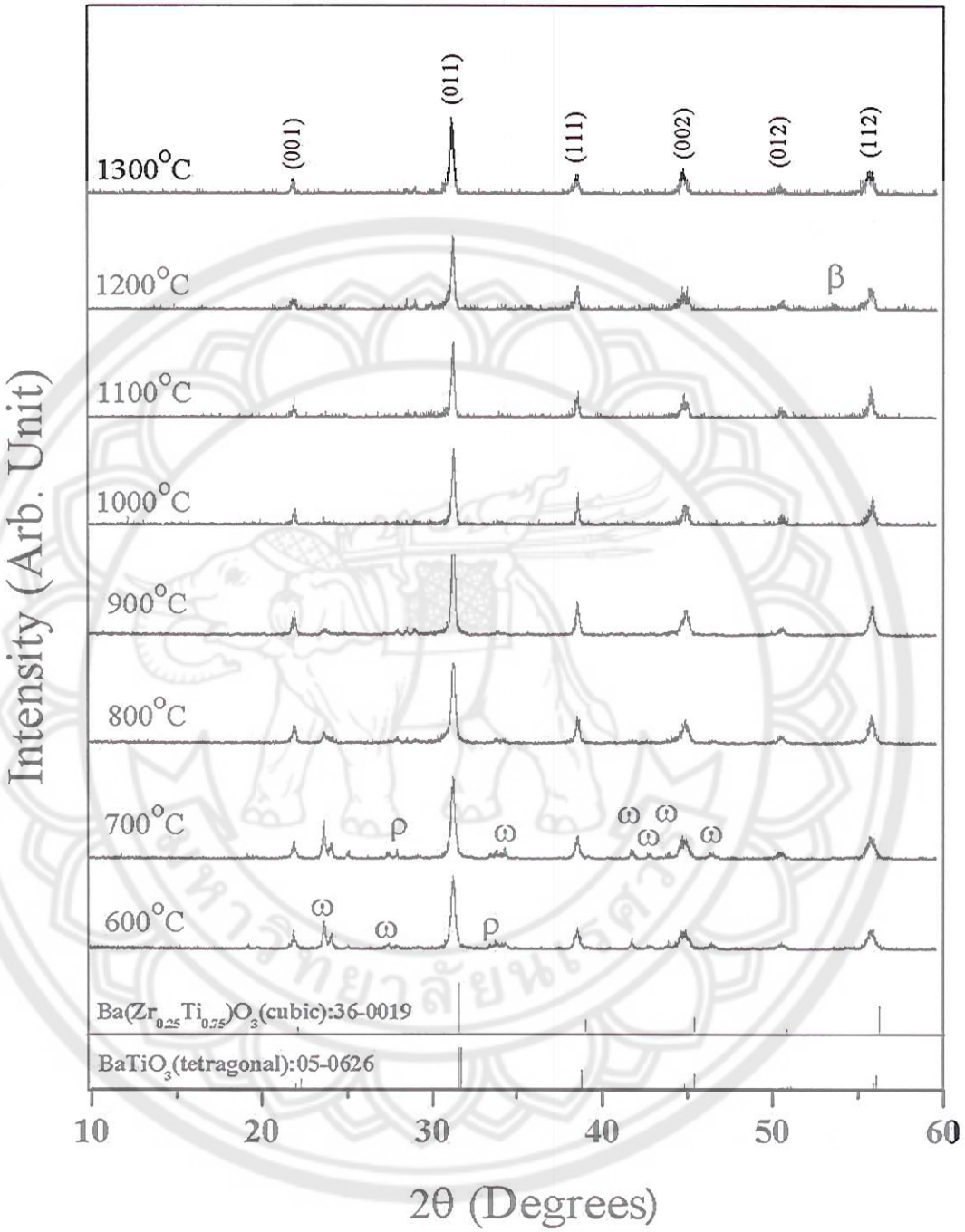

Figure 40 XRD patterns of BZT10 powders calcined at various temperatures for 2 h:(ω) $BaCO_3$; (ρ) ZrO_2; (β) Ba_2TiO_4

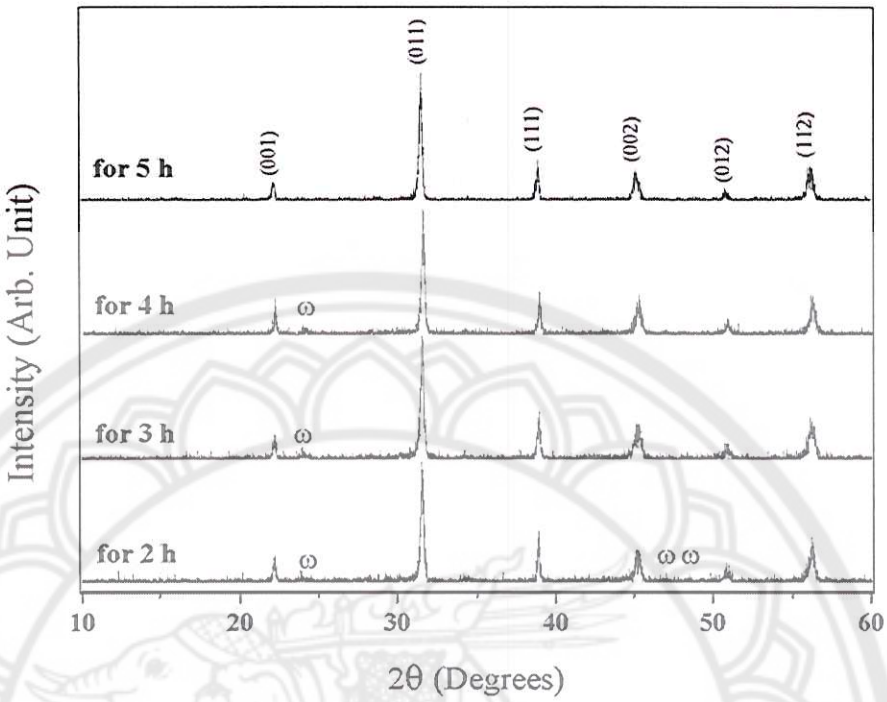

Figure 41 XRD patterns of BZT10 powders calcined at 1000 °C for various dwell times: (ω) $BaCO_3$

Figure 41 shows the XRD patterns of the calcined powder at 1000 °C for 2-5 h. The impurity phase decreased with an increased dwell time and the pure perovskite phase was found in powder calcined at 1000 °C for 5 h. This calcination temperature was lower than that of the solid-state technique by 100-200 °C [6, 8, 10]. This may be caused from the occurrence of combustion energy and the liquid phase which are produced by the melting and decomposing of fuel during combustion process.

Table 10 Percent of perovskite phase and the average particle size of BZT10 powders

Calcination temperature (°C)	Dwell time (h)	% peroveskite	Average particle size (nm)
600	2	33.6	139
700	2	33.7	149
750	2	41.6	171
800	2	69.6	189
850	2	70.4	211
900	2	77.9	224
1000	2	96.5	252
1100	2	94.6	285
1200	2	85.6	333
1300	2	93.1	369
1000	3	96.9	271
1000	4	97.2	292
1000	5	100	298

In terms of the structural phase, Huang, et al. [51] proposed that BZT10 has mixtures of cubic and tetragonal phases with a ratio of 0.5623:0.4377. In this study, the structure of the BZT10 was observed using XRD patterns which measured from 43 to 47° at a very low scanning rate (step size 0.00116°, time/θ 7.42 s, scan speed 0.05152°/s). These are shown in Figure 42. Figure 42(a)-(c) shows the diffraction peak (002) of the BZT10 powders. The diffraction peak changed from non-symmetry (skewed to the right side) to near symmetry when the calcined temperature or dwell time increased. This indicated that the cubic phase content of BZT10 increased with increasing calcination temperatures and dwell time.

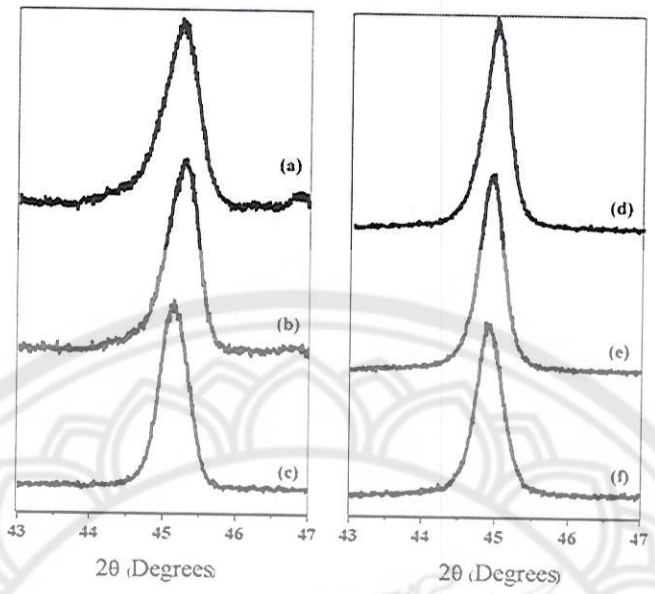

Figure 42 XRD patterns of BZT10 at a very low scanning rate: (a) powder calcined at 800 °C for 2 h, (b) powder calcined at 1000 °C for 2 h, (c) powder calcined at 1000 °C for 5 h, (d) ceramics sintered at 1350 °C for 2 h, (e) ceramics sintered at 1400 °C for 2 h, (f) ceramics sintered at 1450 °C for 2 h

The calcined powders obtained from 1000 °C for 5 h were pressed into pellets and sintered from 1300 to 1500 °C. Figure 43 shows the XRD peak of BZT10 ceramics sintered at 1300-1500 °C for 2 h. A pure perovskite phase was found in all sintered samples. Figure 42 (d)-(f) shows the diffraction peak (002) of the BZT10 ceramics which also indicated that the cubic phase content increased with increasing sintering temperatures. Moreover, the diffraction peak (002) shifted to a lower angle when sintering temperatures increased. The result suggested that the unit cells were stretched with increased sintering temperatures. The effect of firing conditions on the phase formation and lattice parameters of BZT10 may be explained by the variation of the lattice strain and the diffusion process [61, 62]. Eitssayeam, et al. [61] suggested that the increase in firing temperatures influence the lattice strain which determines change in *d* spacing. Moreover, Chen, et al. [62] described the modifications in the lattice parameters and the relative amount of the co-exist phase as a function of firing temperatures which depend on the degree of diffusion which increases the homogenization of the composition.

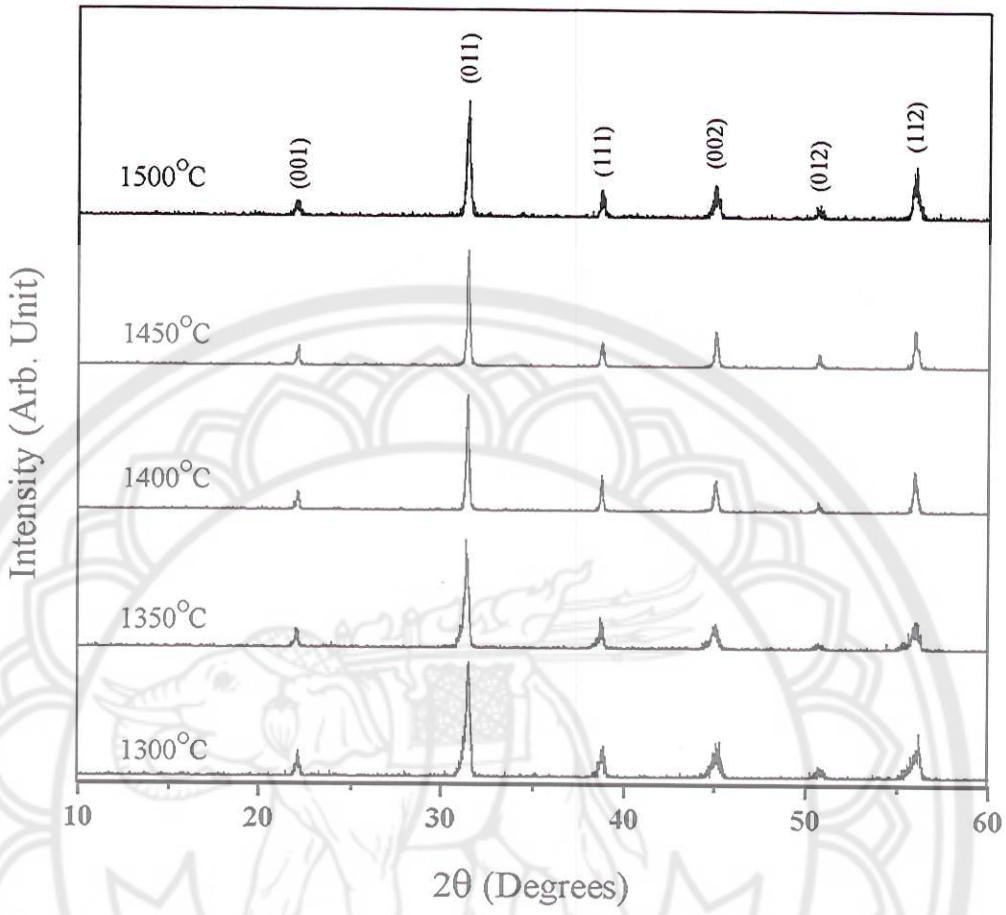

Figure 43 XRD patterns of BZT10 ceramics sintered at various temperatures

The SEM photographs of BZT10 powders calcined between 600 and 1300 °C for 2 h are shown in Figure 44. These powders exhibited an irregular shape and a porous agglomerated form. A narrow particle size distribution was observed at a high calcinations temperature. The average particle size tended to increase in a range of 139-369 nm with increasing calcination temperatures or dwell time as listed in Table 10.

The TEM micrographs of BZT10 calcined powders are shown in Figure 45 and exhibit the agglomerate morphology of BZT10 powders. At low magnification (Figure 47(a)), BZT10 powders showed an agglomerated form and wide agglomerate size distribution in the range of 185-833 nm with an average agglomerate size ~280 nm. They cannot be broken down by ultrasonic agitation which suggests their hard agglomeration. The average agglomerate size observed by the TEM was similar to the

average particle size observed by the SEM. The details of agglomerate morphology were investigated by using higher magnification as seen in Figure 45(b). The image showed agglomerate particles with a diameter around 800 nm and which consisted of irregular shaped particles. In the central region, an opaque zone appeared which was too layered for an electron to be transmitted through. On the edge of the region, electrons partly transmitted through the sample but an accurate particle size could not be observed. The exact crystalline size could be observed by using very high magnification (Figure 45(c)). It could be also seen that many fine particles with a particle size lower than 80 nm existed. This confirms that BZT10 nano-powders can be produced using the combustion technique.

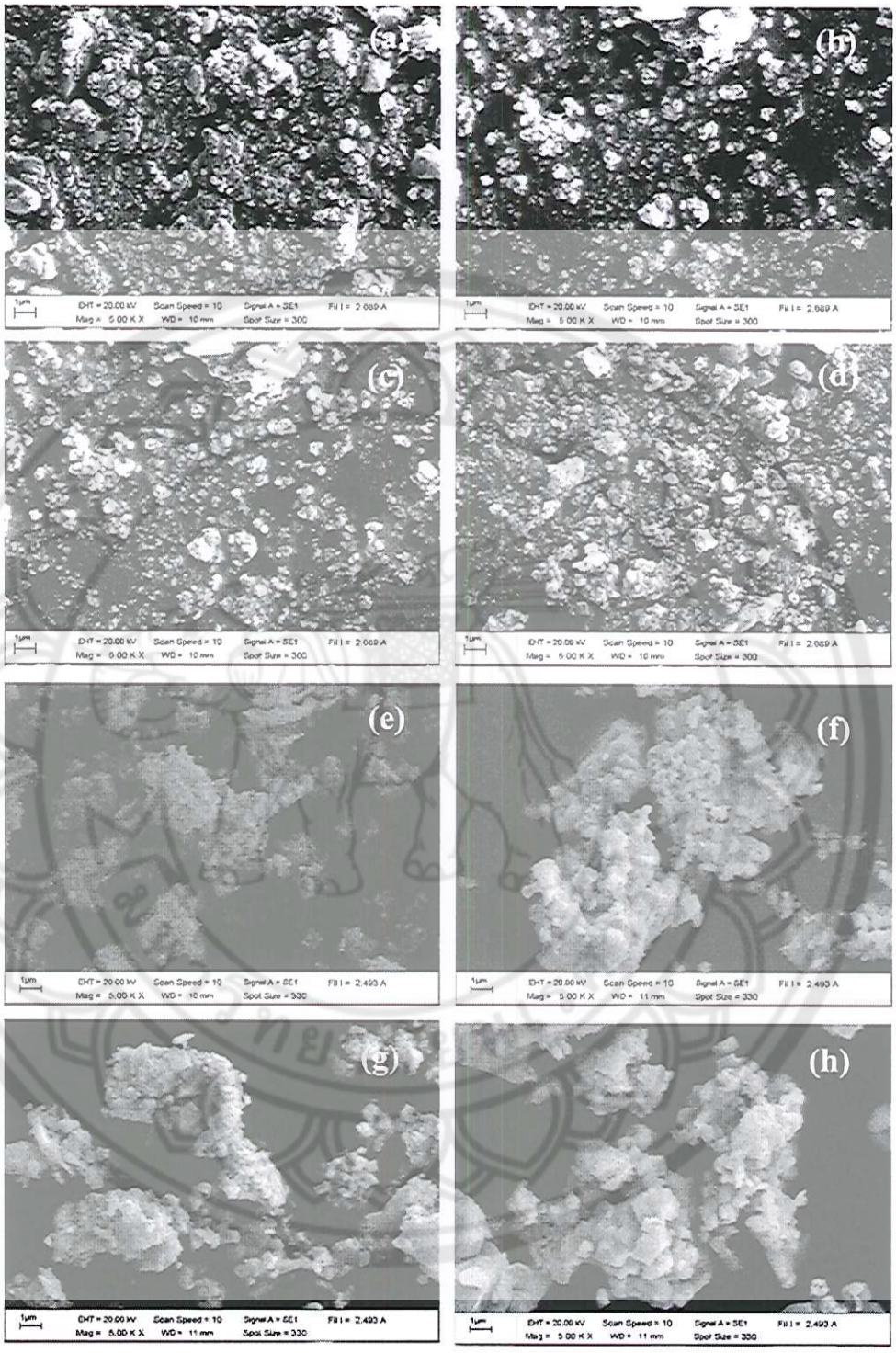

Figure 44 SEM photographs of BZT10 calcined powders for 2 h; (a) calcined at 600 °C, (b) calcined at 700 °C, (c) calcined at 800 °C, (d) calcined at 900 °C, (e) calcined at 1000 °C, (f) calcined at 1100 °C, (g) calcined at 1200 °C and (h) calcined at 1300 °C

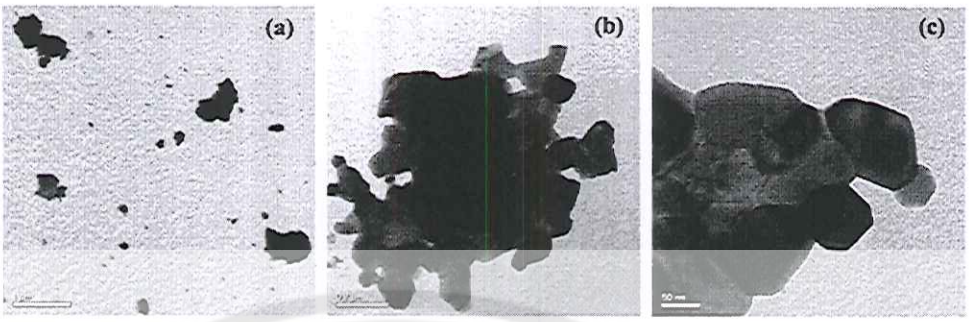

Figure 45 TEM micrographs of BZT10 powders calcined at 1000 °C for 2 h; (a) original magnification x9700, (b) original magnification x46,000, and (c) original magnification x135,000

Figure 46 shows the microstructure of BZT10 ceramics sintered at different temperatures. At a low sintering temperature, the point contacts between particles grew into necks which represented the initial state of sintering (Figure 46(a)). By increasing the sintering temperature, the grain growth became increasingly active and the pore structure collapsed (Figure 46(b) and (c)). In Figure 46(b), the small grains began to melt and large grain boundaries began to emerge. In Figure 46(c), many of the small grains melted together forming larger grains. In Figure 46(d), the grain boundary was melted by high sintering temperatures. This caused the decrease of the grain size and an increase in porosity, respectively. The average grain size is listed in Table 11. The measured density with a variation in sintering temperatures is listed in Table 11. The density of the ceramics was increased when sintering temperatures increased and reached its highest density at 1400 °C. Thereafter, the density decreased when the sintering temperature was higher than 1400 °C. The highest theoretical density via the combustion technique was 97%. This result was higher than the samples which were prepared via the solid-state reaction method (~95%) [10] and the wet chemical reaction method (~96%) [7]. The density results corresponded with microstructure investigation. The increases and decreases in density depended on the porosity and the degree of the liquid phase. According to the phase diagram of BT, the liquid phase started at 1322 °C and increased with the increasing of sintering temperatures [63]. With higher sintering temperatures, the rearrangement of the particles began when the liquid phase occurred and took place rapidly. A sufficient

liquid phase allowed an easy rearrangement of the grains which corresponds to Figure 46(b) and (c). The densification was proportional to the amount of the liquid phase [64]. A large amount of the liquid phase produced an initial rapid densification but a lower final density was the result of void formation due to the evaporation of the materials. As a consequence, the porosity of the pellet increased as seen in Figure 46(d).

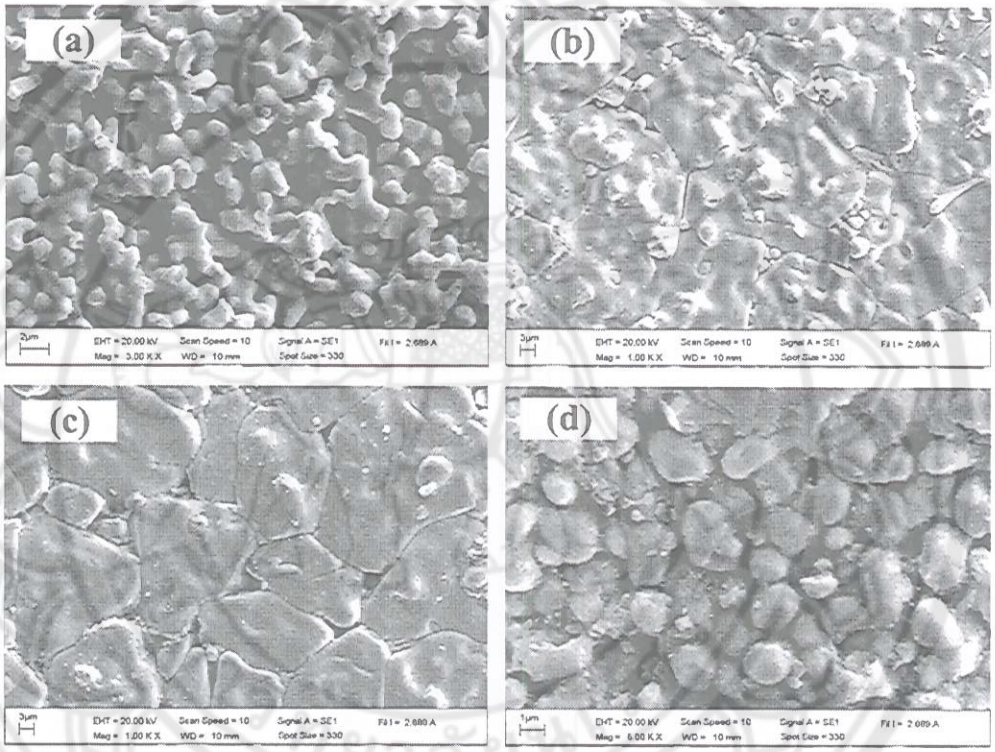

Figure 46 SEM photographs of BZT10 ceramics sintered at; (a) 1300 °C, (b) 1350 °C, (c) 1400 °C, and (d) 1500 °C

Table 11 The average grain size, density, theoretical density, dielectric properties, Curie temperature and diffuseness constant of BZT10 ceramics

Sintered temperature (°C)	Average grain size (μm)	Density (g/cm^3)	Theoretical density (%)	Maximum dielectric constant	Dielectric loss at T_c	T_c (°C)	γ
1300	1.4	5.54	91.6	10,000	0.00208	74.0	1.73
1350	15.2	5.80	96.0	13,000	0.01269	75.5	1.75
1400	21.1	5.84	97.0	16,500	0.01151	75.9	1.76
1450	3.7	5.64	93.3	-	-	-	
1500	1.9	5.05	83.6	-	-	-	

The dielectric curve of BZT10 ceramics with different sintering temperatures for 1 kHz is shown in Figure 47. The dielectric peak corresponded to the Curie temperature (T_c) in which the phase changed from ferroelectric to paraelectric [5, 6]. The Curie temperature increased with an increase of sintering temperatures as listed in Table 11. From previous works, the variation value of T_c of BZT10 ceramics has been reported as: ~105 °C and ~86 °C via the solid state reaction method [6, 65], ~90 °C via the co-precipitation method [7] and ~78 °C via the sol-gel method [9]. In this work, the value of T_c was in a range of 74-76 °C which was lower than in other methods. Kuang ,et al. [8] proposed that a decrease of the T_c on the BZT system was due to the weakening of B-O bonds which depend on the amount of Zr content in the system. The weakening bonds lead to a weaker distortion of the octahedron and a break in the cooperative vibration of B-O chains. This indicated that the combustion method can diffuse Zr ions into barium titanate better than other methods. The diffuseness constant (γ) which describes the diffuseness of the ferroelectric phase transition follows the Curie-Weiss law:

$$\frac{1}{\varepsilon} - \frac{1}{\varepsilon_m} = \frac{(T - T_m)^{\gamma}}{C} \qquad \text{[Eq. 24]}$$

Where ε_m and T_m represent the maximum of dielectric constant and corresponding temperature and C is constant. After plots of $\ln\left(\frac{1}{\varepsilon}-\frac{1}{\varepsilon_m}\right)$ as a function of $\ln(T-T_m)$, the slope of fitting curves is used to determine the γ values. The curve of $\ln\left(\frac{1}{\varepsilon}-\frac{1}{\varepsilon_m}\right)$ versus $\ln(T-T_m)$ of BZT10 sintered between 1300-1400°C are shown in Figure 48. The parameter γ indicates about the character of the phase transition: for $\gamma=1$, a normal Curie-Weiss law and for $\gamma=2$, a complete diffuse phase transition [6]. For $Ba(Zr_xTi_{1-x})O_3$ ceramics, the diffuse transition behavior is enhanced with increasing Zr content [6, 35]. In this work, the γ values of the BZT via the combustion technique is in range of 1.71-1.75 as listed in Table 11. These results were higher than the BZT10 which were prepared via the solid-state reaction method (~ 1.49) [6, 35]. The lower of the T_c and higher of the γ supported that the combustion technique can diffuse Zr ions into barium titanate better than other methods.

The maximum dielectric constant increased with increasing sintering temperatures up to 1400°C and thereafter it decreased (Table 11). The sample sintered at 1500°C could not measure the dielectric constant. The decrease and unmeasurability of the dielectric constant in the samples sintered at high temperatures was due to high porosity which caused a high space charge in the samples. The highest maximum dielectric constant of 16,500 and the lowest dielectric loss 0.0115 were obtained from a sample sintered at 1400°C for 2 h. The dielectric properties corresponded with the density and the microstructure results. Moreover, the higher density and dielectric properties in this study compared to previous works [22, 53, 58], indicated that high quality BZT10 ceramics could prepared via the combustion technique.

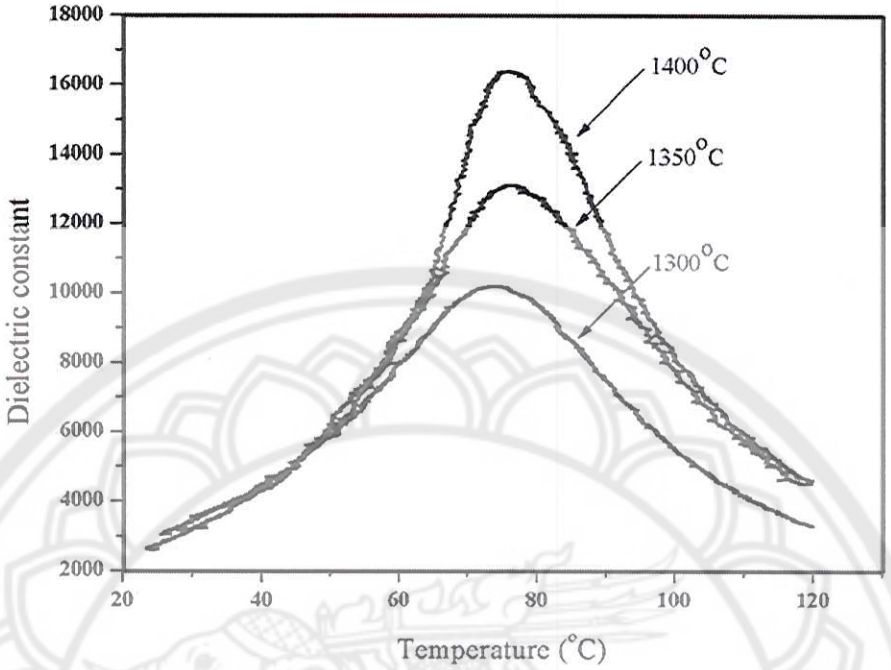

Figure 47 Temperature dependences of dielectric constant of BZT10 ceramics sintered at different temperature

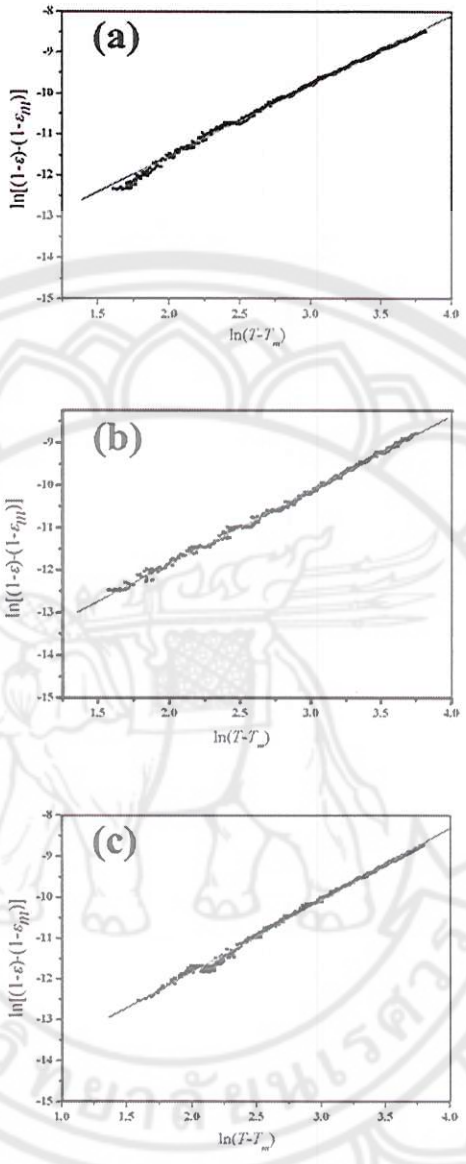

Figure 48 The dependence of $\ln\left(\frac{1}{\varepsilon}-\frac{1}{\varepsilon_m}\right)$ versus $\ln(T-T_m)$ of BZT10 ceramics sintered with various temperatures for 2 h; (a) sintered at 1300 °C, (b) sintered at 1350 °C and (c) sintered at 1400 °C

Conclusions

Low temperature synthesized of pure nano BZT10 powders were performed via the combustion route. The firing conditions influence on phase formation, morphology and dielectric properties of BZT10 ceramics. The phase ratio of

cubic:tetragonal increased with increases of firing temperatures and dwell time. The optimum morphology, highest density, highest dielectric constant, and lowest dielectric loss were obtained from the sample sintered at 1400 °C for 2 h. The Curie temperature occurred around 76 °C, which is lower than BZT10 prepared via other methods. The results of microstructure, densification, and dielectric investigation were supported each others.